

# Fuzzy Logic Direct Torque Control for Asynchronous Motor

JOSÉ LUIS AZCUE, ALFEU J. SGUAREZI FILHO and ERNESTO RUPPERT

Department of Energy Control and Systems

University of Campinas - UNICAMP

Av. Albert Einstein 400, CEP 13083-852

BRAZIL

azcue@ieee.org, sguarezi@dsce.fee.unicamp.br and ruppert@fee.unicamp.br

*Abstract:* - In this article is proposed the Direct Torque Control (DTC) with Space Vector Modulation (SVM) based on Self-Tuning Fuzzy Logic (STFL) controller. This controller determines dynamically the load angle between stator and rotor flux vectors and in consequence the electromagnetic torque necessary to supply the motor load. The rule base for STFL controller is defined in function of the error  $e$  and the change of the error  $\Delta e$  of the torque using a most natural and unbiased membership functions (MF). Constant switching frequency and low torque ripple are obtained using SVM. Performance of the proposed DTC-SVM with STFL are compared with the performance of the same scheme but using PI controller in terms of several performance measures such as settling time, rise time and integral-of-time multiplied by the absolute magnitude of the error index (ITAE). The simulation results show that the proposed scheme can ensure fast torque response and low torque ripple in comparison with DTC-SVM with PI controller.

*Key-Words:* -Direct Torque Control, Space Vector Modulation, Fuzzy Logic Controller, Asynchronous Motor.

## 1 Introduction

The three-phase induction motors (IM) are used in a wide variety of industrial applications due to its simple construction, reliability, robustness and low cost. In the last years DTC has become a popular technique for three-phase IM drives as it provides a fast dynamic torque response and robustness under machine parameter variations without the use of current regulators, e.g., voltage-vector selection using switching table [1] and direct self-control [2], however, nowadays exist some other alternative DTC schemes to reduce the torque ripples using the Space Vector Modulation (SVM) technique [3][4].

In [5] it is presented a simple one step stator flux control algorithm which avoids coordinate rotation and predictive controllers. However, this scheme needs a good adjustment of the PI torque controller parameters to achieve a good performance. In general the use of fuzzy control does not require the accurate mathematic model of the process to be controlled. Instead, it uses the experience and knowledge of the involved professionals to construct its control rule base.

Fuzzy logic has been proved to be powerful in the motor control area, e.g., in [6] the PI and Fuzzy Logic Controllers (FLC) are used to control the load angle which simplifies the IM drive system. In [7] the FLC is used to obtain the reference voltage

vector dynamically in terms of torque error, stator flux error and stator flux angle. In this case both torque and stator flux ripples are remarkably reduced. Another paper on fuzzy logic application in DTC-SVM shows that the fuzzy PI (or PI-type fuzzy) speed controller has a better response for a wide range of motor speed [8]. Different type of adaptive FLC such as self-tuning and self-organizing controllers has also been developed and implemented [9].

In [10] it was used a self-tuning PI-type fuzzy controller to control a second-order linear and marginally stable system. This method requires three scaling factors (SF) or gains. The performance analysis of this controller was compared to the regular PI controller and the results were very encouraging. The same was done in [11] where the self-tuning PI-type fuzzy controller was used in an industrial weigh belt feeder control process successfully. In both cases only the output scaling factor was adjusted online depending on the process trend.

In this paper it was designed a STFL for a DTC-SVM three-phase IM based in [5], where only the output controller gain (output SF) was adjusted continuously with the help of fuzzy rules considering that it is equivalent to the controller gain. It has been given the highest priority to the output SF tuning due to its strong influence on the performance and stability of the system.

In our scheme, the STFL generates corrective control actions based on the real torque trend only. This controller was tuned dynamically online during the control operation by adjusting its output SF by a gain updating factor  $\alpha$ . The value of  $\alpha$  is determined from a fuzzy rule base defined in function of the control error  $e$  and in the variations of the control error  $\Delta e$  as shown in the tables provided in the paper body and derived from the knowledge of the control process.

According to the torque error  $e$  and to the change of torque error  $\Delta e$ , the required load angle is provided by a STFL. With this angle thereference stator flux is calculated and the stator voltage vector necessary for tracking the reference torque is synthesized.

The simulation results show that the proposed STFL controller for the DTC-SVM three-phase IM outperforms the same scheme with conventional PI [5].

The paper is organized as follows. In section 2 the basic control principles of the three-phase induction motor DTC is presented. In section 3 the topology of the proposed control scheme is analyzed and in section 4 the proposed STFL is described in details mentioning different aspects of its design consideration.

Section 5 presents the simulations results of STFL controller performance in comparison with the conventional PI controller. Both controllers were applied to three-phase induction motor DTC-SVM scheme. Finally, conclusion is given in Section 6.

## 2 Basic Control Principles

### 2.1 Dynamic Equations of the Three-Phase Induction Motor

By utilizing the definitions of the fluxes, currents and voltages space vectors, the dynamic equations of the three-phase IM in stationary reference frame can be put into the following mathematical form [12]:

$$\vec{u}_s = R_s \vec{i}_s + \frac{d\vec{\psi}_s}{dt} \quad (1)$$

$$0 = R_r \vec{i}_r + \frac{d\vec{\psi}_r}{dt} - j\omega_r \vec{\psi}_r \quad (2)$$

$$\vec{\psi}_s = L_s \vec{i}_s + L_m \vec{i}_r \quad (3)$$

$$\vec{\psi}_r = L_r \vec{i}_r + L_m \vec{i}_s \quad (4)$$

Where  $\vec{u}_s$  is the stator voltage space vector,  $\vec{i}_s$  and  $\vec{i}_r$  are the stator and rotor current space vectors, respectively,  $\vec{\psi}_s$  and  $\vec{\psi}_r$  are the stator and rotor flux space vectors,  $\omega_r$  is the rotor angular speed,

$R_s$  and  $R_r$  are the stator and rotor resistances,  $L_s$ ,  $L_r$  and  $L_m$  are the stator, rotor and mutual inductance, respectively.

The electromagnetic torque is expressed in terms of the cross product of the stator and the rotor flux space vectors.

$$t_e = \frac{3}{2} P \frac{L_m}{L_r L_s \sigma} \vec{\psi}_r \times \vec{\psi}_s \quad (5)$$

$$t_e = \frac{3}{2} P \frac{L_m}{L_r L_s \sigma} |\vec{\psi}_r| |\vec{\psi}_s| \sin(\gamma) \quad (6)$$

Where  $\gamma$  is the load angle between stator and rotor flux space vectors,  $P$  is the number of pole pairs of the motor and  $\sigma = 1 - L_m^2 / (L_s L_r)$  is the dispersion factor.

### 2.2 Three-phase Induction Motor Direct Torque Control

In the direct torque control if the sample time is short enough, such that the stator voltage space vector is imposed to the motor keeping the stator flux constant at the reference value, the rotor flux can be considered constant because it changes slower than the stator flux. The electromagnetic torque (6) can be quickly changed by changing the angle  $\gamma$  in the desired direction. This angle  $\gamma$  can be easily changed when choosing the appropriate stator voltage space vector.

For simplicity, let us assume that the stator phase ohmic drop could be neglected in (1). Therefore  $d\vec{\psi}_s/dt = \vec{u}_s$ . During a short time  $\Delta t$ , when the voltage space vector is applied, it has:

$$\Delta \vec{\psi}_s \approx \vec{u}_s \cdot \Delta t \quad (7)$$

Thus the stator flux space vector moves by  $\Delta \vec{\psi}_s$  in the direction of the stator voltage space vector at a speed which is proportional to the magnitude of the stator voltage space vector. By selecting step-by-step the appropriate stator voltage vector, it is possible to change the stator flux in the required direction.

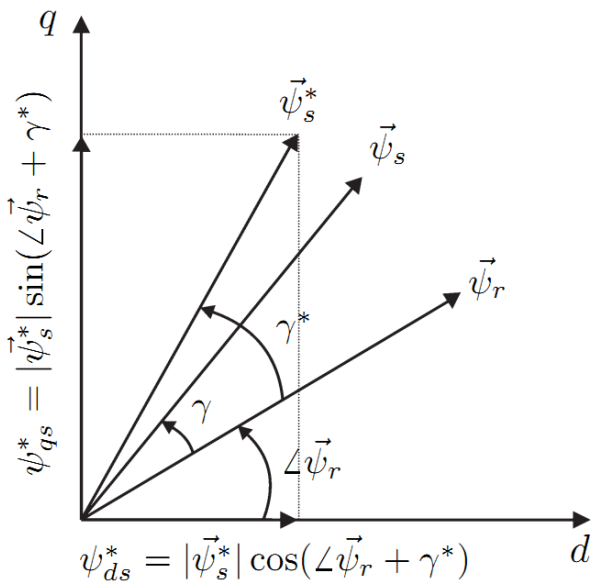


Fig.1. Load angle  $\gamma^*$  between reference stator flux  $\vec{\psi}_s^*$  and rotor flux  $\vec{\psi}_r$  in stationary reference frame.

### 3 Direct Torque Control with Space Vector Modulation

Fuzzy logic control has been proved to be powerful and able to solve many IM control problems. In Fig. 2 we show the block diagram for the Direct Torque Control with Space Vector Modulation scheme and STFL controller, this scheme is an alternative to the classical DTC schemes presented in [1], [2] and [3]. In this scheme, the next load angle  $\gamma^*$  is not prefixed but it is determinate by the STFL controller. The equation (6) shows that the angle  $\gamma$  determines the electromagnetic torque which is necessary to supply the load. The proposed STFL determines the load angle from the torque error  $e$  and the change of torque error  $\Delta e$ . Details about this controller are going to be presented in the next section.

In Fig. 3, it can be seen the scheme of the power electronics drive used in our simulation. The control signals for the three-phase with two-level inverter are generated by the proposed DTC-SVM scheme shown in Fig. 2.

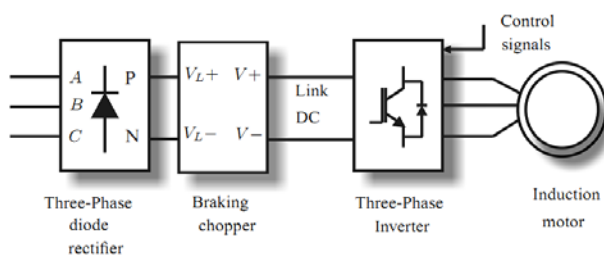


Fig.3. Power electronics drive scheme.

### 3.1 ReferenceStator Flux Calculation

As shown in Fig. 1, in stationary reference frame, the stator flux reference  $\vec{\psi}_s^*$  can be decomposed in two perpendicular components  $\psi_{ds}^*$  and  $\psi_{qs}^*$ . The addition of the angle  $\gamma^*$ , which is the output of the STFL, with the estimated rotor flux angle  $\Delta\psi_r$  permits to estimate the next value of reference stator flux angle.

In this paper, the magnitude of reference stator flux is considered constant ( $|\vec{\psi}_s^*| = \text{rated flux}$ ). It uses the relation presented in (8) to calculate the reference stator flux vector [5].

$$\vec{\psi}_s^* = |\vec{\psi}_s^*| \cos(\gamma^* + \Delta\psi_r) + j |\vec{\psi}_s^*| \sin(\gamma^* + \Delta\psi_r) \quad (8)$$

With the application of the stator voltage  $\vec{u}_s$  during a short time  $\Delta t$  it is possible to reproduce a flux variation  $\Delta\vec{\psi}_s$ . Notice that the stator flux variation is nearly proportional to the stator voltage space vector as seen in the equation (7).

### 3.2 Stator Voltage Calculation

The stator voltage space vector is in function of the DC link voltage ( $U_{dc}$ ) and the inverter switch state ( $S_a, S_b, S_c$ ).

The stator voltage vector  $\vec{u}_s$  is determined as in [13] by:

$$\vec{u}_s = \frac{2}{3} \left[ \left( S_a + \frac{S_b + S_c}{2} \right) + j \frac{\sqrt{3}}{2} (S_b - S_c) \right] U_{dc} \quad (9)$$

### 3.3 Space Vector Modulation Technique

In this work is used the space vector modulation (SVM) technique with the aim to reduce the torque ripple and total harmonic distortion of the current, it is therefore necessary to understand the operation and fundamentals that governing their behavior. This concept was discussed in publications such as [14], [15] and [16]. For our purpose the basic ideas are summarized.

In Fig. 4 is shown the three-phase two level inverter diagram, where the state of the switches follow the following logic.

$$S_{wi} = \begin{cases} 1, & \text{the switch } S_{wi} \text{ is turn ON and } \bar{S}_{wi} \text{ is turn OFF} \\ 0, & \text{the switch } S_{wi} \text{ is turn OFF and } \bar{S}_{wi} \text{ is turn ON} \end{cases}$$

Where  $i = a, b, c$ .

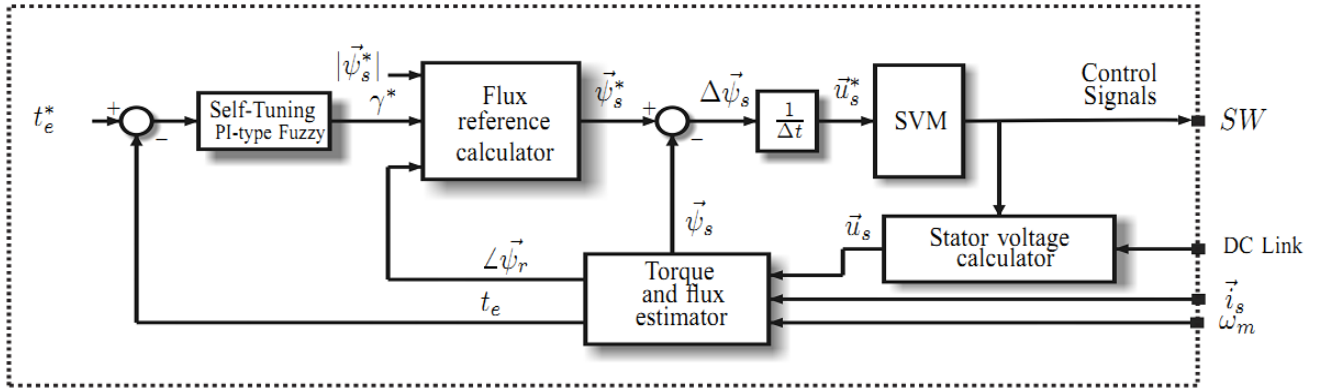


Fig.2. Self-tuning fuzzy logic direct torque control block diagram.

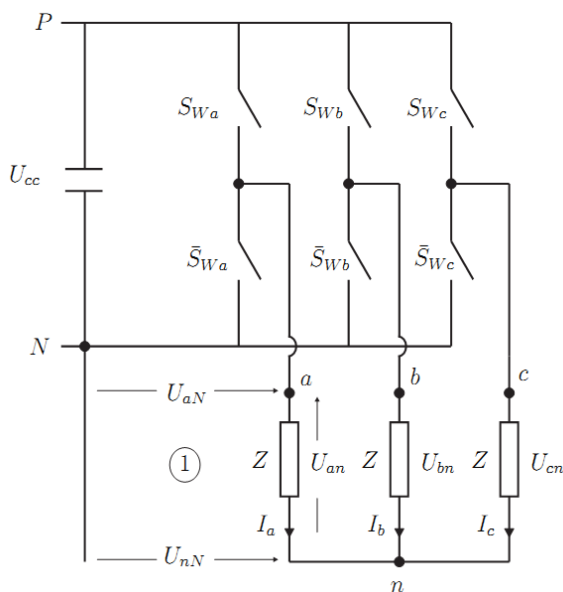


Fig.4. Three-phase two level inverter with load.

Where the switch  $\bar{S}_{Wa}$  is the complement of  $S_{Wa}$ , then is possible to resume all the combinations only considering the top switches as is shown in Table 1.

Where  $\vec{S}_0, \vec{S}_1, \vec{S}_2, \vec{S}_3, \vec{S}_4, \vec{S}_5, \vec{S}_6$  and  $\vec{S}_7$  are switching vectors. Between these switching vectors we have six active voltage vectors ( $\vec{U}_1, \vec{U}_2, \vec{U}_3, \vec{U}_4, \vec{U}_5$  and  $\vec{U}_6$ ) and two zero voltage vectors ( $\vec{U}_0$  and  $\vec{U}_7$ ) as is shown in Fig. 5.

The generalized expression to calculate the active and zero vectors is:

$$\vec{U}_n = \begin{cases} \frac{2}{3} \sqrt{3} U_{dc} \cdot e^{j(2n-1)\frac{\pi}{6}}, & n = 1, \dots, 6 \\ 0 & , n = 0, 7 \end{cases} \quad (10)$$

Table 1. Switching vectors

Vector	$S_{Wa}$	$S_{Wb}$	$S_{Wc}$
$\vec{S}_0$	0	0	0
$\vec{S}_1$	1	0	0
$\vec{S}_2$	1	1	0
$\vec{S}_3$	0	1	0
$\vec{S}_4$	0	1	1
$\vec{S}_5$	0	0	1
$\vec{S}_6$	1	0	1
$\vec{S}_7$	1	1	1

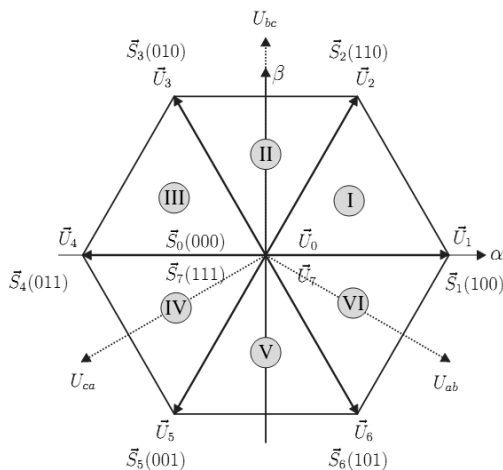


Fig.5. Relations between voltage and switching vectors.

In Fig. 5 the hexagon is divided in six sectors, and any reference voltage vector is represented as combination of adjacent active vectors and zero vectors, e.g. the voltage vector  $\vec{U}^*$  is localized in sector I between active vectors  $\vec{U}_1$  and  $\vec{U}_2$ , as is shown in Fig. 6, and considering a enough short switching period, it is:

$$\vec{U}^* = \vec{U}_1 \frac{T_1}{T_z} + \vec{U}_2 \frac{T_2}{T_z} \quad (11)$$

The times  $T_1$  and  $T_2$  are calculated using trigonometric projections as is shown in Fig. 6, it is:

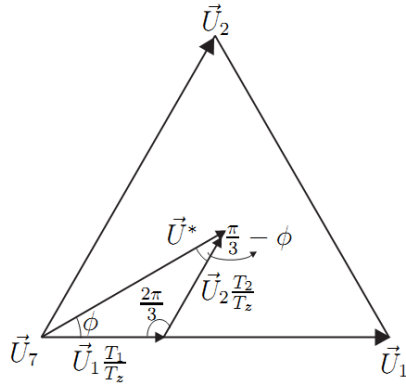


Fig.6. Reference stator voltage ( $\vec{U}^*$ ) in sector I.

$$T_1 = \frac{|\vec{U}^*|}{|\vec{U}_1|} T_z \frac{\sin(\frac{\pi}{3} - \phi)}{\sin(\frac{2\pi}{3})} \quad (12)$$

$$T_2 = \frac{|\vec{U}^*|}{|\vec{U}_2|} T_z \frac{\sin(\phi)}{\sin(\frac{2\pi}{3})} \quad (13)$$

Where  $T_1$  and  $T_2$  are the times of application of the active vectors in a switching period,  $T_z$  is the switching period,  $\phi$  is the angle between the reference voltage vector and adjacent active vector ( $\vec{U}_1$ ).

If the sum of times  $T_1$  and  $T_2$  is minor of the switching period, the rest of the time is apply the zero vectors, it is:

$$T_0 = T_7 = T_z - T_1 - T_2 \quad (14)$$

Where  $T_0$  and  $T_7$  are the times of applications of zero vectors in a switching period.

The next step is to follow a specific switching sequence, this one depends if the reference vector is localized in an even or odd sector, e.g. in Fig. 8 is observed the optimum switching sequence for odd sector ( $\vec{S}_0, \vec{S}_1, \vec{S}_2$  and  $\vec{S}_7$ ), however for even sector the switching sequence is contrary to the case for odd sector.

In Fig. 8 is observed the pulse pattern when the reference voltage vector is localized in an odd sector, this pattern is knowledge as symmetrical pattern.

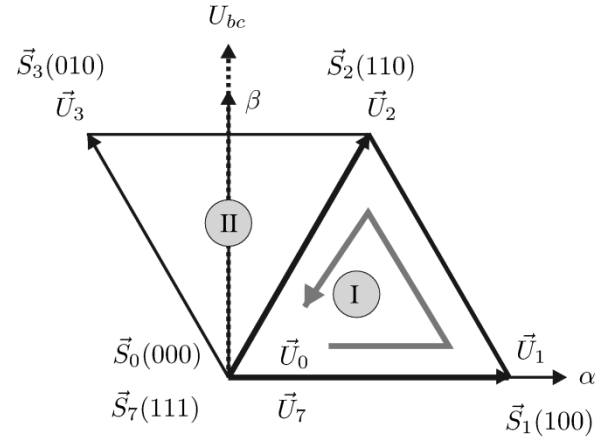


Fig.7. Switching sequence for odd sector.

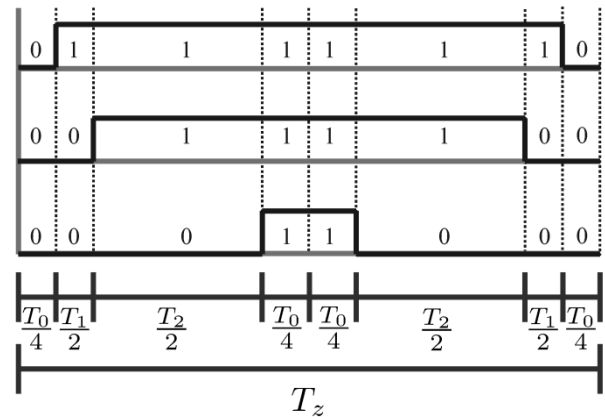


Fig.8. Pulse pattern of space vector modulation for odd sector.

### 3.4 Torque and Stator Flux Estimation

The electromagnetic torque and the stator flux are estimated using the stator voltage and the stator current space vectors, therefore:

$$\vec{\psi}_s = \int (\vec{u}_s - R_s \vec{i}_s) dt \quad (15)$$

On the other hand, the rotor flux depends on the stator flux estimated and stator current space vectors. The rotor flux space vector can be estimated from equations (3) and(4), it is:

$$\vec{\psi}_r = \frac{L_r}{L_m} \vec{\psi}_s - \frac{L_s L_r}{L_m} \sigma \vec{i}_s \quad (16)$$

With the components of  $\vec{\psi}_r$ , we can obtain the angle of the rotor flux:

$$\angle \vec{\psi}_r = \tan^{-1} \left( \frac{\psi_{rq}}{\psi_{rd}} \right) \quad (17)$$

The stator and rotor fluxes given by the equations (15) and(16) respectively are substituted in (5) to estimate the motor electromagnetic torque.

### 4 Design of self-tuning fuzzy logic controller

The STFL controller proposed which is depicted in Fig. 9 is composed by a PI-type fuzzy (PIF) controller and gain tuning fuzzy (GTF) controller, as well as two input scale factors ( $G_e, G_{\Delta e}$ )and one output scale factor ( $G_{\gamma^*}$ ). Finally it has the saturation block to limit the output.

The STFL controller has only a single input variable, which is the torque error  $e$ , and one output variable which is the motor load angle  $\gamma^*$  given by:

$$\gamma^*(k) = \gamma^*(k - 1) + \Delta\gamma^*(k) \quad (18)$$

In (18),  $k$  is the sampling time and  $\Delta\gamma^*(k)$ represents the incremental change of the controller output. It is emphasized here that the accumulationof the controller output takes place out of the fuzzy part of the controller and it does not influences the fuzzy rules.

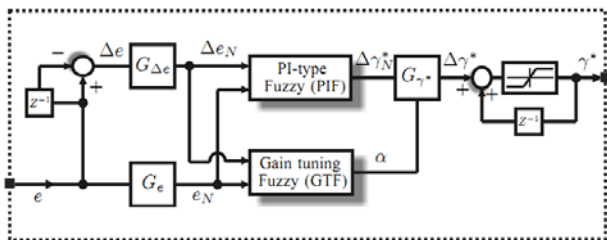


Fig.9. Self-tuning fuzzy logic controller

#### 4.1 Membership Functions

The membership functions for PIF controller are shown in Fig. 10, these membership functions (MF's) are the same for input variables  $e_N$  and  $\Delta e_N$ , and output variable  $\Delta\gamma_N^*$ . Observe that the universe of discourse of these fuzzy sets is normalized in the closed interval [-1,1].

The MF's for GTF controller are shown in Fig. 10 and Fig. 11 for the input and output variables respectively. The universe of discourse for the input variables ( $e_N$ and $\Delta e_N$ ) are defined in the closed interval [-1,1] and for the output variable ( $\alpha$ ) are defined in the closed interval [0,1].

The great part of the MF's have triangular shapes as is shown in Fig. 10 and in Fig. 11 with

50% overlapping neighbor functions, except the extremes which are trapezoidal MF's. The linguistic variables are referred to as: NL-Negative Large, NM-Negative Medium, NS-Negative Small, ZE-Zero, PS-Positive Small, PM-Positive Medium, PL-Positive Large for the Fig. 10and as ZE-Zero, VS-Very Small, S - Small, SL - Small Large, ML - Medium Large, L – Large and VL -Very Large for the Fig. 11.

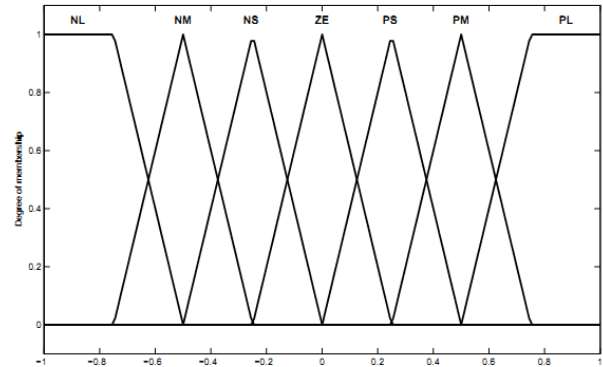


Fig.10. Membership functions for  $e_N, \Delta e_N$  and  $\Delta\gamma_N^*$ .

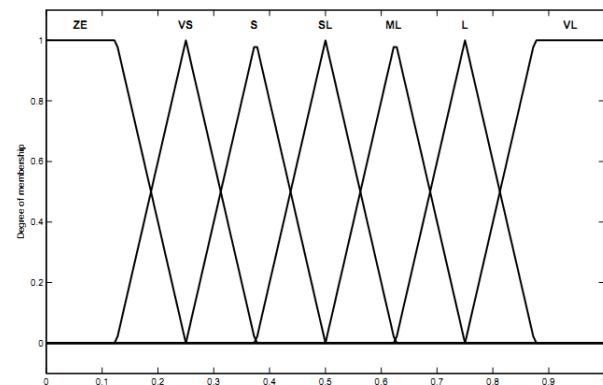


Fig.11. Membership functions for  $\alpha$  output

#### 4.2 Scaling Factors

It is adopted two Scaling Factors (SF's) for the inputs with fixed values ( $G_e$  and  $G_{\Delta e}$ ),and one SF for the output ( $G_{\gamma^*}$ ) as is shown in Fig. 12. The output SF value can be adjusted dynamically through updating the  $\alpha$  factor, this factor is computed online by using a model independent fuzzy rules defined in terms of  $e_N$  and  $\Delta e_N$ . The relationship between the SF's and the input/output variables of the STFL controller are shown below:

$$e_N = G_e \cdot e \quad (19)$$

$$\Delta e_N = G_{\Delta e} \cdot \Delta e \quad (20)$$

$$\Delta\gamma^* = (\alpha \cdot G_{\gamma^*}) \cdot \Delta\gamma_N^* \quad (21)$$

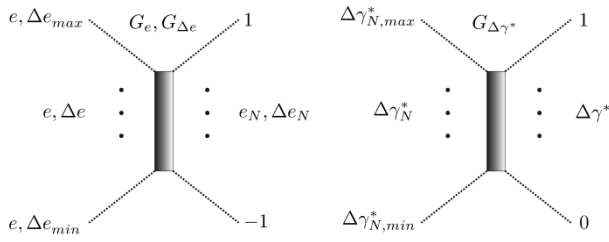


Fig.12. Input and output scaling factors.

### 4.3 The Rule Bases

The incremental change in the PIF controller output ( $\Delta\gamma_N^*$ ) is determined by the rules of the form:

$$R_x: \text{if } e_N \text{ is } E \text{ and } \Delta e_N \text{ is } \Delta E \text{ then } \Delta\gamma_N^* \text{ is } \Delta\Gamma_N^* \quad (22)$$

Where  $\Delta E = E = \Delta\Gamma_N^* = \{NL, NM, NS, ZE, PS, PM, PL\}$ . The output  $\alpha$  for the GTF controller is determined by the rules of the form:

$$R_y: \text{if } e_N \text{ is } E \text{ and } \Delta e_N \text{ is } \Delta E \text{ then } \alpha \text{ is } A \quad (23)$$

Where  $E = \Delta E = \{NL, NM, NS, ZE, PS, PM, PL\}$  and  $A = \{ZE, VS, S, SL, ML, L, VL\}$ . The rule bases to calculate  $\Delta\gamma_N^*$  and  $\alpha$  are shown in Table 2 and in Table 3 respectively.

Table 2. Fuzzy rules for computation of  $\Delta\gamma_N^*$

$\Delta e_N/e_N$	NL	NM	NS	ZE	PS	PM	PL
NL	NL	NL	NL	NM	NS	NS	ZE
NM	NL	NM	NM	NM	NS	ZE	PS
NS	NL	NM	NS	NS	ZE	PS	PM
ZE	NL	NM	NS	ZE	PS	PM	PL
PS	NM	NS	ZE	PS	PS	PM	PL
PM	NS	ZE	PS	PM	PM	PM	PL
PL	ZE	PS	PS	PM	PL	PL	PL

Table 3. Fuzzy rules for computation of  $\alpha$

$\Delta e_N/e_N$	NL	NM	NS	ZE	PS	PM	PL
NL	VL	VL	VL	L	SL	S	ZE
NM	VL	VL	L	L	ML	S	VS
NS	VL	ML	L	VL	VS	S	VS
ZE	S	SL	ML	ZE	ML	SL	S
PS	VS	S	VS	VL	L	ML	VL
PM	VS	S	ML	L	L	VL	VL
PL	ZE	S	SL	L	VL	VL	VL

### 4.4 Gain Tuning Fuzzy Controller

The target of the GTF controller is online continuous update the value of  $\alpha$  in every sample time. The  $\alpha$  value is necessary to control the percentage of the output SF ( $G_{\gamma^*}$ ) that will be apply to  $\Delta\gamma_N^*$  and finally calculate the new  $\Delta\gamma^*$ , therefore:

$$\Delta\gamma^* = (\alpha \cdot G_{\gamma^*}) \cdot \Delta\gamma_N^* \quad (24)$$

The GTF controller rule base is based on the knowledge about the three-phase IM control, using a DTC type control according to the scheme proposed in [5], in order to avoid large overshoot and undershoot, e.g., in Fig. 13 is observed a step response of the electromagnetic torque, when  $e$  and  $\Delta e$  have different signs, it means that the torque estimated  $t_e$  is approaching to the reference torque  $t_e^*$ , then the output SF  $G_{\gamma^*}$  must be reduced to a small value by  $\alpha$ , for instance, if  $e$  is PM and  $\Delta e$  is NM then  $\alpha$  is S.

On the other hand, when  $e$  and  $\Delta e$  have the same sign, it means that the estimated torque  $t_e$  is moving away from the reference torque  $t_e^*$ , the output SF  $G_{\gamma^*}$  must be increased to a large value by  $\alpha$  in order to correct the torque direction quickly and avoid that the torque departs from the reference torque, for instance, if  $e$  is PM and  $\Delta e$  is PM then  $\alpha$  is VL, as is observed in Table 3.

The control surfaces of the PIF controller and GTF controller are shown in Fig. 14 and Fig. 15 respectively. In Fig. 14 is shown the nonlinear relationship between the inputs and output variables ( $e, \Delta e$  and  $\Delta\gamma_N^*$ ) and in Fig. 15 is shown the nonlinear relationship between  $e$  and  $\Delta e$  inputs, and  $\alpha$  output, the Fig. 16 shows the same control surface of Fig. 15 but rotated in order to better observe the details of this surface.

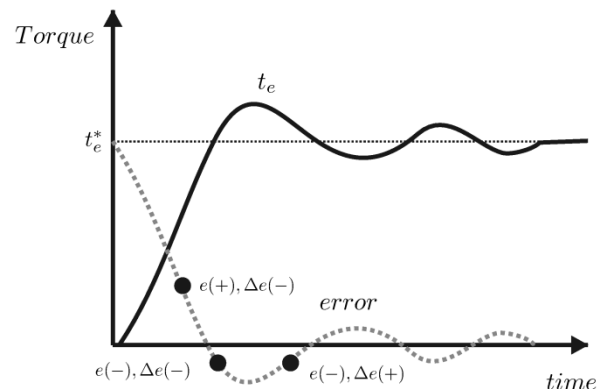




Fig.13. Step response of the electromagnetic torque.

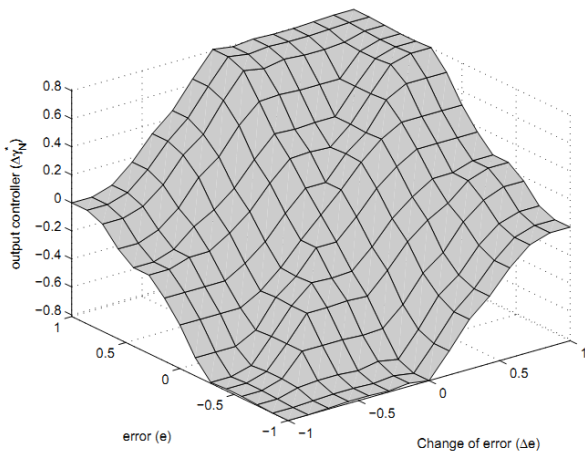


Fig.14. Control surface of self-tuning fuzzy logic controller output ( $\Delta\gamma_N^*$ ).

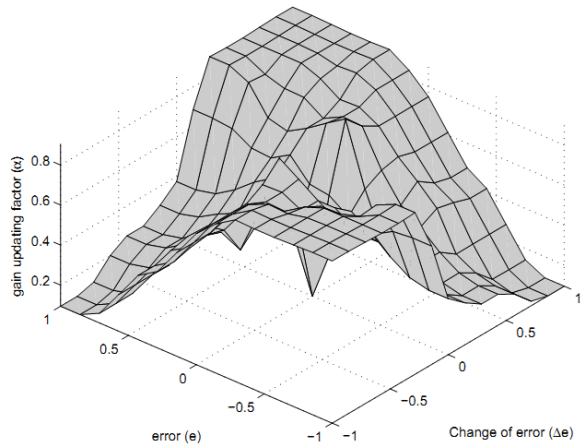


Fig.15. Control surface of gain tuning fuzzy controller output ( $\alpha$ ).

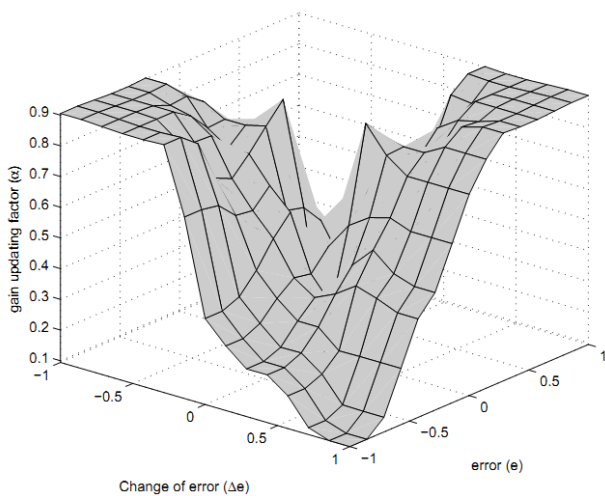


Fig.16. Control surface of gain tuning fuzzy controller output ( $\alpha$ ) (rotated).

The inference method used in this article is the Mamdani's implication based on max-min aggregation and center of area method is used for defuzzification.

### 5 Simulation Results

The simulations were performed using MATLAB environment with Simulink blocksets and fuzzy logic toolbox. The switching frequency considered for the three-phase two level inverter was 10kHz. The three-phase induction motor parameters are given in Table 5 and the reference stator flux considered was 0.47 Wb which is the rated stator flux of this IM.

In order to investigate the effectiveness of the proposed control system and in order to check the closed-loop stability of the complete system, it was performed several tests.

It was used different dynamic operating conditions such as step change in the motor, no load sudden change in the reference speed and finally was applied a specific load torque profile.

The Fig. 17 and Fig.18 show similar behaviors of the torque, current and the motor speed when it is imposed a no-load reference speed step change from 0.5 pu to -0.5 pu in the DTC-SVM scheme with STFL and PI controllers respectively. The sinusoidal shape of the current shows that this control technique leads also a good current control, in other words this means that the current control is inherent to the algorithm control presented in this work.

The Fig. 19 presents the results when the same torque profile is imposed to DTC-SVM scheme with STFL and with the PI controller, this test was made when the motor is operating at 90 percent of rated speed. In both cases the controllers follow the reference torque.

The Fig. 20 illustrates that the DTC-SVM scheme with PI controller and the proposed scheme have similar dynamic response to step change in the motor load. In Table 4 it can be seen that the rise time  $t_r$ , the settling time  $t_s$  and the integral of time multiplied by the absolute magnitude of the error index (ITAE) were relatively smaller in the proposed scheme when compared to the scheme with PI controller, very well adjusted. It could be seen that the DTC-SVM scheme with STFL controller is faster than the DTC-SVM scheme with PI controller.

The simulation results show that the proposed STFL controller for the DTC-SVM three-phase IM outperforms the same scheme with conventional PI [5], validating the proposed scheme.



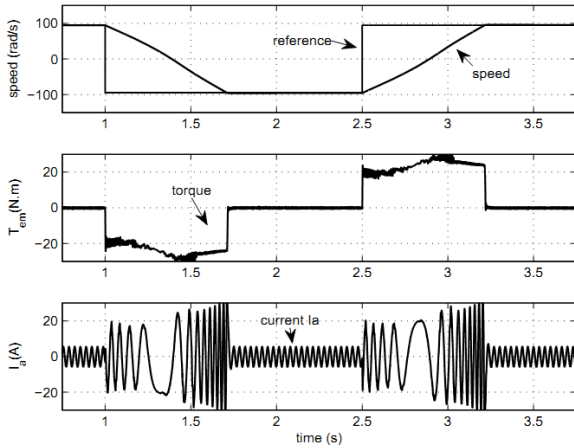


Fig.17. Step change in the reference speed for DTC-SVM with STFL controller.

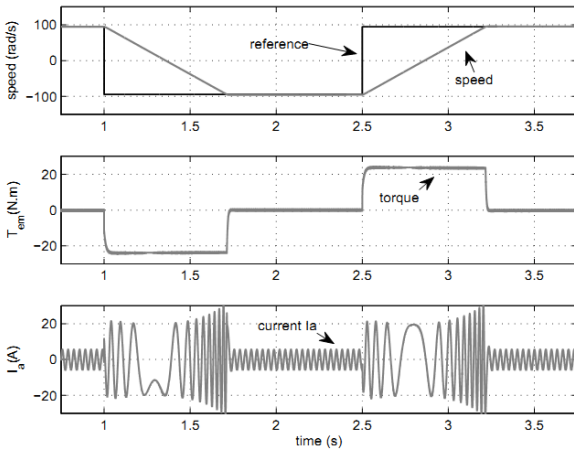


Fig.18. Step change in the reference speed for DTC-SVM with PI controller

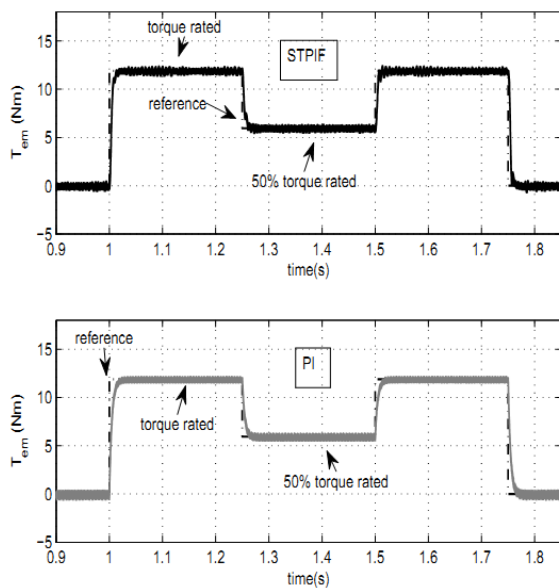


Fig.19. Torque profile for DTC-SVM with STFL and PI controller.

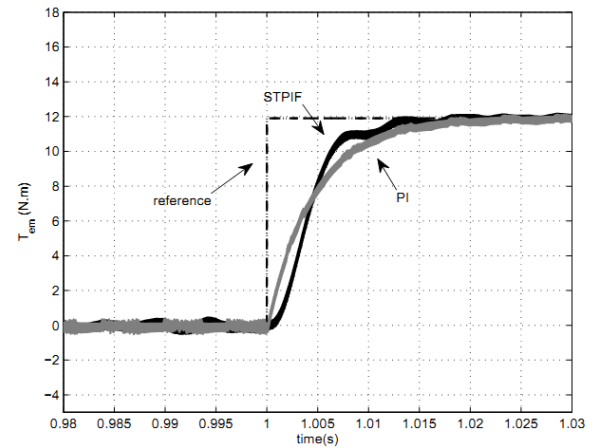


Fig.20. Step change in torque for DTC-SVM scheme with STFL and PI controller.

Table 4. Performance measures

	$t_r(ms)$	$t_s(ms)$	ITAE
DTC-SVM PI	9,53	16,0	212,8
DTC-SVM STFL	5,49	12,0	199,5

Table 5. Induction motor parameters[17]

Rated voltage (V)	220/60 Hz
Rated power (HP)	3
Rated torque (N.m)	11,9
Rated speed (rad/s)	179
$R_s, R_r (\Omega)$	0,435; 0,816
$L_{ls}, L_{lr} (H)$	0,002; 0,002
$L_m (H)$	0,0693
$J (Kg m^2)$	0,089
P (pair of poles)	2

## 6 Conclusion

In this paper it was presented the DTC-SVM scheme to control a three-phase IM using a STFL controller. This scheme was used in order to determine dynamically and online the load angle between stator and rotor flux space vectors. This load angle and the rotor flux angle estimated determine the reference stator flux and in consequence it was synthesized the stator voltage space vector necessary to track the reference torque.

Simulations at different operating conditions have been carried out. The simulation results verify that the proposed DTC-SVM scheme with STFL controller achieves a fast torque response and low torque ripple, in comparison to the DTC-SVM scheme with PI controller, in a wide range of operating conditions such as sudden change in the command speed, reverse operation and step change of the load.

## References:

- [1] I. Takahashi and T. Noguchi, "A new quick-response and high-efficiency control strategy of an induction motor," *Industry Applications, IEEE Transactions on*, vol. IA-22, no. 5, pp. 820–827, sept. 1986.
- [2] M. Depenbrock, "Direct self-control (dsc) of inverter-fed induction machine," *Power Electronics, IEEE Transactions on*, vol. 3, no. 4, pp. 420–429, oct 1988.
- [3] T. Habetler, F. Profumo, M. Pastorelli, and L. Tolbert, "Direct torque control of induction machines using space vector modulation," *Industry Applications, IEEE Transactions on*, vol. 28, no. 5, pp. 1045–1053, 1992.
- [4] J.-K. Kang and S.-K. Sul, "New direct torque control of induction motor for minimum torque ripple and constant switching frequency," *Industry Applications, IEEE Transactions on*, vol. 35, no. 5, pp. 1076–1082, 1999.
- [5] J. Rodriguez, J. Pontt, C. Silva, S. Kouro, and H. Miranda, "A novel direct torque control scheme for induction machines with space vector modulation," in *Power Electronics Specialists Conference, 2004. PESC 04. 2004 IEEE 35th Annual*, vol. 2, june 2004, pp. 1392–1397 Vol.2.
- [6] H. Abu-Rub, J. Guzinski, Z. Krzeminski, and H. Toliyat, "Advanced control of induction motor based on load angle estimation," *Industrial Electronics, IEEE Transactions on*, vol. 51, no. 1, pp. 5–14, feb. 2004.
- [7] L. Chen, K.-L. Fang, and Z.-F. Hu, "A scheme of fuzzy direct torque control for induction machine," in *Machine Learning and Cybernetics, 2005. Proceedings of 2005 International Conference on*, vol. 2, aug. 2005, pp. 803–807 Vol. 2.
- [8] Z. Koutsogiannis, G. Adamidis, and A. Fyntanakis, "Direct torque control using space vector modulation and dynamic performance of the drive, via a fuzzy logic controller for speed regulation," *Power Electronics and Applications, 2007 European Conference on*, pp. 1–10, sept. 2007.
- [9] Y.-M. Park, U.-C. Moon, and K. Lee, "A self-organizing fuzzy logic controller for dynamic systems using a fuzzy auto-regressive moving average (farma) model," *Fuzzy Systems, IEEE Transactions on*, vol. 3, no. 1, pp. 75–82, feb 1995.
- [10] R. Mudi and N. Pal, "A robust self-tuning scheme for pi- and pd-type fuzzy controllers," *Fuzzy Systems, IEEE Transactions on*, vol. 7, no. 1, pp. 2–16, feb 1999.
- [11] Y. Zhao and J. Collins, E.G., "Fuzzy pi control design for an industrial weigh belt feeder," *Fuzzy Systems, IEEE Transactions on*, vol. 11, no. 3, pp. 311–319, june 2003.
- [12] P. Vas, *Sensorless Vector and Direct Torque Control*. Oxford University Press, 1998, ISBN 0198564651.
- [13] M. Bertoluzzo, G. Buja, and R. Menis, "A direct torque control scheme for induction motor drives using the current model flux estimation," *Diagnostics for Electric Machines, Power Electronics and Drives, 2007. SDEMPED 2007. IEEE International Symposium on*, pp. 185–190, sept. 2007.
- [14] H. van der Broeck, H.-C. Skudelny, and G. Stanke, "Analysis and realization of a pulsewidth modulator based on voltage space vectors," *Industry Applications, IEEE Transactions on*, vol. 24, no. 1, pp. 142–150, 1988.
- [15] J. Holtz, "Pulsewidth modulation-a survey," *Industrial Electronics, IEEE Transactions on*, vol. 39, no. 5, pp. 410–420, oct 1992.
- [16] K. Zhou and D. Wang, "Relationship between space-vector modulation and three-phase carrier-based PWM: a comprehensive analysis [three-phase inverters]," *Industrial Electronics, IEEE Transactions on*, vol. 49, no. 1, pp. 186–196, 2002.
- [17] P. C. Krause, O. Wasynczuk, and S. D. Sudhoff, *Analysis of Electric Machinery and Drive Systems*. IEEE Press, 2002.